Taylor & Francis
Taylor & Francis Group

Combustion Theory and Modelling

ISSN: 1364-7830 (Print) 1741-3559 (Online) Journal homepage: www.tandfonline.com/journals/tctm20

Model reduction of chemical kinetics via decomposition: SPVF theory and ILDM-based initial data projection

Viatcheslav Bykov & Vladimir Goldshtein

To cite this article: Viatcheslav Bykov & Vladimir Goldshtein (31 Mar 2026): Model reduction of chemical kinetics via decomposition: SPVF theory and ILDM-based initial data projection, Combustion Theory and Modelling, DOI: 10.1080/13647830.2026.2647067

To link to this article: https://doi.org/10.1080/13647830.2026.2647067

Published online: 31 Mar 2026.

Combustion Theory and Modelling, 2026
https://doi.org/10.1080/13647830.2026.2647067

Model reduction of chemical kinetics via decomposition: SPVF theory and ILDM-based initial data projection

Viatcheslav Bykov [a*] and Vladimir Goldshtein[b]

[a]*Karlsruhe Institute of Technology, Karlsruhe, Germany* [b]*Department of Mathematics, Ben-Gurion University of the Negev, Beer–Sheva, Israel*

(*Received 9 July 2025; accepted 8 March 2026*)

This study outlines and discusses model reduction problems. The concept of Singularly Perturbed Vector Fields (SPVF) is revisited as a framework for handling the decomposition of motions and, in particular, for addressing the fundamental problem of initial-data consistency in reduced models. This issue arises because the initial conditions generally do not lie on the slow invariant manifold that approximates the reduced system. To address this, this study demonstrates how the method of Intrinsic Low-Dimensional Manifolds (ILDMs) can be employed both to approximate the slow manifold and to generate consistent initial data. Two classical benchmark examples in model reduction theory are examined to verify and discuss the approach. The Lindemann mechanism is used to illustrate how SPVF theory reconciles the standard asymptotic limits and thereby captures both pressure dependence and variations in reaction order. The Michaelis–Menten model serves as a key example where standard reduction approaches – such as QSSA and PEA – may fail under certain asymptotic conditions. The SPVF framework provides a systematic way to understand these limitations by clarifying the asymptotic structure and its parameter dependencies. Meanwhile the ILDM method not only offers an efficient way to approximate the slow manifold but also supplies consistent initial data projection procedure, ensuring a physically and mathematically sound reduced system.

Keywords: Mechanisms of chemical kinetics; model reduction; singular perturbations; slow/fast invariant manifolds; initial data projection

1. Introduction and motivation

The problem of model reduction has attracted an increasing attention in the recent decades due to the progress made in numerical computations, which became a valuable tool in scientific research, industry and engineering [1–3]. The usage of numerical integration packages and increase of role of computations not only in engineering but also in science has extended the range of applications for modelling leading both to improvement and to growth in the complexity of combustion models and to the extension of experimental data for model validation. The collected data have become complex in terms of dimension, while models developed grow both in dimension and in stiffness especially with respect to considered chemical kinetic models [4].

There are two main reasons for this. One concerns the internal property of combustion processes which are highly sensitive to, e.g. temperature and species

*Corresponding author. Email: viatcheslav.bykov@kit.edu

concentration variations, etc. This is manifested by the fact that combustion is typically localised/concentrated phenomena in space and in time. As a result, the chemically reacting source terms become highly non-linear with respect to parameters and variables used to model the chemical reactions. Hence, modelling of such processes with given accuracy becomes challenging [5].

Another reason is relevant to the way chemical kinetic models have been developing. Typically one starts with simple several steps models that describe certain phenomena with a given accuracy. Then the scope of the phenomena changes and one intends to account for wide parameters/regimes/configurations range to describe additional phenomena and experimental evidences. This is typically performed by an extension of the original chemical reaction network by adding steps to the original set of elementary reactions. This has been implemented capturing additional phenomena successfully; however, such an extension must not degrade the performance of the original model in its initial application range. Thus an extension can only be realised if the added sub-models effectively cancel out while being implemented in the original regime. The system then becomes artificially over-determined and stiff.

To cope with the problem of overdetermination of mathematical models with the focus on a limited application range, numerous model reduction techniques have been developed over the past few decades as referenced in [6, 7]. Their primary goal is to automatically decrease the number of system variables within the model, while ensuring that the performance remains largely unaffected.

All these approaches can be roughly subdivided into two groups. The first is based on so-called progress variables, parameters (e.g. flamelets [8]) while methods in the second group rely on multiple time scales (ILDM [9], CSP [10], REDIM [11], etc.).

Methods belonging to the first group concern specific regime/configuration only assuming the initial data is limited and rely solely on the detailed solutions for a reacting system being automatically invariant as the system solution. The reduced system state is then considered to be constrained to the detailed solution trajectory/profile started at the confined set of initial data. A significant hurdle with application of these approaches is in selecting initial conditions and boundary conditions for distributed systems such that the representative states are obtained to constrain the system that will accurately capture the detailed system behaviour. If the chosen initial/boundary data are not representative and assumption is not valid, then the reduced model might not accurately capture the system's dynamics across its intended application range.

Methods in the second group [10] are based on the intrinsic property of existing multiple time scales and are, therefore, independent of any additional assumption. They can be implemented for an arbitrary initial state and only need to provide the appropriate projection of the initial state onto so-called low-dimensional manifolds. A valuable advantage of such approaches based on time-scale separation is that they reduce not only the dimension but also the stiffness of the original mathematical model. Main methods of this group are based on a local time scale analysis [9, 10]. Although such approaches are preferable they might also have shortcomings in applications. For instance, different time scale divisions for the same set of parameters in different subdomains, 'ghosts' low-dimensional manifolds as approximation of the slow invariant manifold, which have nothing to do with the slow manifold and require special tools for their recognition [12].

As it turns out, both groups (and likely any other existing model reduction approach) rely on low-dimensional manifolds. However, these manifolds differ significantly both in their construction and properties when addressing the model reduction problem. In the

first group, manifolds usually have a dimension equal to that of the 'initial data set' plus a number of progress variables. The methods in the second group rely on manifolds that depend on the internal structure of the time scale hierarchy present in the system. Being based on attractive slow manifolds, they remain stable with respect to small perturbations. To address these assumptions and formalise the fast/slow separation, the theory of Singularly Perturbed Systems (SPSs) has been established [13]. This theory can be utilised once the decomposition is known and explicit.

In applications, especially for relatively high-dimensional systems, deriving a dimensionless form using already known key parameters that control time scale differences analytically is possible, but not realistic. Therefore, an automatic procedure that can perform this task is of primary importance both to with respect finding characteristic time scales, key system parameters as well as to find out appropriate SPS form (proper dimensionless form) of the engineering scale problem. The question then arises as – what should be done if the system is presented in a dimensional form, and neither key parameters nor variables governing the different time scales are known.

The first methods to address this problem were ILDM (Intrinsic Low-Dimensional Manifold) [9] and CSP (Computational Singular Perturbation) [10]. Both assume that time scale separation is present in the system, can be defined locally, and that asymptotic limits are valid across the range of initial data and system parameters. A discrete spectral gap of the non-linear source term is typically used for this purpose [14].

The theory of coordinate-free singular perturbations, known as Singularly Perturbed Vector Fields (SPVF) [15], was developed to extend the standard theory of singular perturbations. It formulates the main question of model reduction for over-determined systems that are represented as singularly perturbed vector fields.

The SPVF theory answers several important questions relevant to defining the hidden small system parameter, identifying regular and singular vector field components, and understanding the structure and dimension of fast fibers as manifolds for fast motions and base sets – slow manifolds [14, 15]. These serve as a substitute for the standard SPS coordinates. This knowledge becomes crucial for the description of fast manifolds, and it is necessary to evaluate attractive slow manifolds, and it helps correctly project arbitrary initial states onto these slow manifolds.

Additionally, these insights are also required to clarify in detail the attractiveness property of the slow manifolds, which are intended for model reduction. The SPVF's theoretical basis for model reduction, founded on multiple time scales, has been established to address all implementation-relevant questions and the treatment of related problems. From a pure mathematical point of view, the main purpose of the SPVF method is to identify a fiber bundle structure of the original model in the systems' state space and, if possible, transform it into a standard SPS system through a corresponding change of variables.

In cases where such a transformation is linear – meaning the fast fibers have a linear structure – the theory simplifies to applying the standard SPS framework to the transformed systems. To evaluate the corresponding linear transformation, the Global Quasilinearisation Procedure (GQL approach) has been developed [14]. This paper presents suggested ideas and highlights the importance of the extended singular perturbation theory (SPVF) for the successful description and application of multiple-time-scale-based approaches. It begins with a brief revision of the standard SPS theory, outlining the major steps in SPVF development. This is important for self-consistency.

Next, two basic benchmark examples from model reduction theory are revisited: the Lindemann (LD) [16] and Michaelis–Menten (MM) [17, 18] models. In the case of the LD

model, a linear transformation to the original model exists and can be used to delineate two important asymptotical limits for describing pressure-dependent reactions. The MM model, even in appropriate asymptotical limits, presents difficulties with implementing standard model reduction tools like the quasi-steady-state assumption (QSSA) [19, 20]. In this scenario, non-linear fibers become evident and can be approximated by the ILDM fast subspace. The analytical study performed demonstrates how SPVF theory augmented with the ILDM approximation of fast manifolds can overcome difficulties of initial data projection in applications with a weak asymptotic limit.

2. Singularly perturbed vector fields (SPVF)

Before a detailed analysis of the reduced model applications to the Lindemann mechanism and the Michaelis–Menten enzyme kinetics the main idea and concept behind the SPVF method is outlined shortly. Let us start from the standard SPS system [13, 21],

$$\frac{\mathrm{d}x}{\mathrm{d}t} = F(x, y), \quad \frac{\mathrm{d}y}{\mathrm{d}t} = \varepsilon G(x, y). \tag{1}$$

Here, $x \in \mathbf{R}^n$, $y \in \mathbf{R}^m$ correspondingly fast and slow variables, $\varepsilon << 1$, $F(x, y)$ and $G(x, y)$ are of the same order. The first equation is the fast equation and the second one is the slow equation. The fast null-cline is a zero approximation of the corresponding slow invariant manifold. Let $z := (x, y)$ and $\Phi(z, \varepsilon) := (F(z), \varepsilon\, G(z))$.

A coordinate-free description of the zero approximation of the slow invariant manifold is given by $\Phi(z, 0) = F(z) = 0$. The rank of the Jacobi matrix $J_{\Phi(z,0)}$ is less or equal to n that is the dimension of the fast motions. These basic considerations have leaded to the concept of SPVFs [15, 22].

In many cases, the existence of a small parameter ε and the decomposition of the vector field into slow and fast sub-fields are not known. Therefore this coordinate-free definition can be useful. Let $\Phi(z) := F(z) + \epsilon G(z)$ where all vector functions $F, G, \Phi : \mathbf{R}^{n+m} \to \mathbf{R}^{n+m}$. Here, $F(z)$ is the fast subfield and $G(z)$ is the slow subfield. The classical zero approximation $\epsilon \to 0$ is $\Phi(z) = F(z)$. Two main cases are possible: a non-degenerate and a degenerate and the standard SPS is an example of a degenerate one.

In the non-degenerate system dimension of the slow set $F(z) = 0$ is zero (typically a number of isolated points). This corresponds to a regularly perturbed vector field Φ.

In the so-called degenerate case, dimension of the zero set M of all solutions of equation $F(z) = 0$ is not zero. This corresponds to a 'singularly perturbed' vector field Φ. Under additional assumption that all vector fields are smooth it is possible that the set M is a combination of manifolds of different dimensions. This special case is very complex and, thus, an additionally assumption that M is a manifold of a fixed dimension – m has been made.

2.1. *Degenerate vector fields*

This case corresponds to the theory of Singularly Perturbed Vector Fields (SPVF) [22]. For systems with such vector fields slow invariant manifolds exist. The determination of the degeneracy of a vector field represents a complex problem and relatively simple cases are discussed here.

Let us return to the case $\Phi(z) := F(z) + \epsilon G(z)$ where $\Phi : \mathbf{R}^{n+m} \to \mathbf{R}^{n+m}$, where $J_\Phi(z)$ denotes Jacobi matrix of the fast vector field

$$J_\Phi(z) = \frac{\partial \Phi(z)}{\partial z}, \quad J_\Phi(z)_{\varepsilon \to 0} = \frac{\partial F(z)}{\partial z}. \tag{2}$$

The assumption about the generation of the fast vector field made leads to the fact that the rank of this matrix has to be constant and equals to n. Consequently, the dimension of the slow manifold is equal to m, and the dimension of the 'fast motion' is equal to n.

Consider now $z \in M$ and take a union of all trajectories S_z of the fast vector field – $F(z)$ that pass through z. These will be so-called a fast fibers – manifolds associated with the point $z \in M$. In general, these fibers can vary significantly from point to point, and the overall situation can become quite complex. Conditions for existence and properties of slow manifolds and of fiber bundles of the Singularly Perturbed Vector Field (SPVF) can be found in [23]. Once the decomposition is known and a new coordinate system that transforms an original model into a singularly perturbed one is found, the problem of model reduction can be stated as being converted to the well-studied and settled theory of singularly perturbed systems (Equation 1). This theory can then be used to reduce the model and reduce the dynamics of the system either on the fast fibers/manifolds or constrain them to the evolution within the slow manifold.

There are other complex issues with manifolds-based model reduction. These can occur when a slow manifold has degenerate solution branches, or when those branches lose stability and attractiveness with respect to the fast manifolds. The first issue relates to situations where formal solutions exist but might be nonphysical [12] or leave the physical domain (e.g. species concentrations become negative). In the second case, the system's solution trajectory will not tend toward such an unstable branch of the manifold, and the formal usage of such branches can lead to unpredictable errors. These complex issues are much more delicate, typically relevant to situations where a particular asymptotic limit is already in question, and remain beyond the scope of this study. The reader is referred to [6, 13, 23] for more details on the subject.

An automatic procedure for the decomposition of the vector field Φ onto slow and fast parts is developed only under assumption that the corresponding fiber bundle is a priori vector bundle. From the brief outline above, one can conclude that the level of degeneracy and the particular asymptotic limit can be determined and tested by investigating the system Jacobi matrix, as suggested in the ILDM [9]. Thus the decomposition structure and the fast/slow vector fields can be approximated via relevant eigenspaces of the system Jacobi matrix similar as in [14].

3. Lindemann model

To illustrate the idea and to demonstrate how useful a suggested combination might be both at the analytical and computational levels, the Lindemann model is considered first. This simple weakly non-linear model is a classic example that highlights the importance of a comprehensive, global approach to obtain system decomposition, which might account for different asymptotic limits automatically.

In his classic paper, Lindemann used his model to successfully explain several gas phase decomposition reactions that do not follow first-order uni-molecular kinetics ($A \longrightarrow P$), but rather exhibit higher (up to the second) order kinetics. He also addressed the question

of the energy required for molecular decomposition to sustain the flame propagation [24]. Lindemann established the appropriate mechanism by introducing an excited and an inert species:

$$\begin{aligned} A + M &\rightleftharpoons A^* + M \\ A^* &\longrightarrow P. \end{aligned} \tag{3}$$

Here, A specifies the reactant, A^* specifies its excited form, P is the product and M is an inertial body (third body) concentration. The low mass action leads to the quadratic form of the first reaction rate (Equation 3), $\psi = (A, M, A^*, P)$:

$$\begin{aligned} R_1(\psi) &= k_1^+[A][M] - k_1^-[A^*][M], \\ R_2(\psi) &= k_2^+[A^*]. \end{aligned} \tag{4}$$

The fact that only two reactions exist, the rank of stoichiometry matrix is only two (see appendix Subsection A.1) gives us two linearly independent equations of the system, which are trivially decoupled. The limits of high and low pressure can now be investigated by using standard model reduction assumption, e.g. QSSA with the natural choice of A^* as radical – fast variable in the plane (A, A^*):

$$\begin{aligned} \frac{\mathrm{d}[A]}{\mathrm{d}t} &= -R_1(\psi) = -k_1^+[A][M] + k_1^-[A^*][M], \\ \frac{\mathrm{d}[A^*]}{\mathrm{d}t} &= R_1(\psi) - R_2(\psi) = k_1^+[A][M] - k_1^-[A^*][M] - k_2^+[A^*]. \end{aligned} \tag{5}$$

However, the obvious choice to represent the system equation (5) would be the choice of variables – (A, P):

$$\begin{aligned} \frac{\mathrm{d}[A]}{\mathrm{d}t} &= -R_1(\psi) = -k_1^+[A][M] + k_1^-[A^*][M] = \\ &\quad - k_1^+[A][M] + k_1^-[M](C_0 - [A] - [P]), \\ \frac{\mathrm{d}[P]}{\mathrm{d}t} &= R_2(\psi) = k_2^+[A^*] = k_2^+(C_0 - [A] - [P]). \end{aligned} \tag{6}$$

This is because in this form, both reactions are decoupled. They can then be individually compared and used to define an appropriate dimensionless form, depending on which reaction is dominating in the considered limit. Then the standard Singularly Perturbed Systems (SPS) theory can be applied for the analysis, as shown below.

3.1. *Well-known high and low pressure asymptotic limits*

Application of both standard approximations – QSSA and PEA – can be justified by using standard theory of singularly perturbed system accompanied by proper scaling the time variable.

3.1.1. *Standard QSSA*

The activated species A^* plays a role of radical in the detailed mechanism, thus it is logical to treat it as a fast variable. This means that in this process the quasi-equilibrium for A^*

$$\frac{\mathrm{d}[A^*]}{\mathrm{d}t} \sim 0 \Rightarrow k_1^+[A][M] - k_1^-[A^*][M] - k_2^+[A^*] = 0, \tag{7}$$

defines the slow manifold approximation and thus the system can be reduced using this constraint.

This leads to a simplified form of the corresponding equation for the product formation (Equation 6) depending on the educt concentration (Equation 7)

$$\frac{\mathrm{d}[P]}{\mathrm{d}t} = R_2(\psi) = k_2^+ \frac{k_1^+[A][M]}{k_1^-[M] + k_2^+}. \tag{8}$$

Different limits of the rates k_1^+, k_1^-, k_2^+, provide

- First order for high-pressure limit

$$k_1^-[M] >> k_2^+ \Rightarrow \frac{\mathrm{d}[P]}{\mathrm{d}t} = k_2^+[A^*] = k_2^+ \frac{k_1^+[A][M]}{k_1^-[M] + k_2^+} \approx \frac{k_1^+ k_2^+}{k_1^-}[A]; \tag{9}$$

- The non-linear dependence of the concentration expressed as $[A]^\alpha$, $\alpha \neq 1$, is observed for low pressure limit. This occurs when the complicated dependence of the third body $-M$ on A, A^* due to e.g. linear integrals is taken into account, namely:

$$k_1^-[M] << k_2^+ \Rightarrow \frac{\mathrm{d}[P]}{\mathrm{d}t} = k_2^+[A^*] = k_2^+ \frac{k_1^+[A][M]}{k_1^-[M] + k_2^+} \approx k_1^+[A][M]. \tag{10}$$

3.1.2. *Standard PEA*

Because the only one elementary reaction (i.e. reversible one) is present, partially equilibrium of this only reaction means

$$R_1(\psi) = k_1^+[A][M] - k_1^-[A^*][M] \sim 0 \Rightarrow [A^*] = \frac{k_1^+}{k_1^-}[A]. \tag{11}$$

By applying this particular assumption, the only one limit (Equation 9) can be recovered due to $[A^*] = \frac{k_1^+}{k_1^-}[A]$. Still the observed in the experiments higher order dependencies in A can be nevertheless attained when an additional assumption of quasi-steady state of this reaction is made, namely,

$$\frac{\mathrm{d}R_1(\psi)}{\mathrm{d}t} = k_1^+ \frac{[A]}{\mathrm{d}t}[M] - k_1^- \frac{[A^*]}{\mathrm{d}t}[M] \sim 0 \tag{12}$$

Theoretically, this corresponds to a higher order of approximation of the corresponding slow invariant manifold of the system leading to more accurate predictions with an additional factor of $\frac{k_1^+}{k_1^-}$

$$\frac{\mathrm{d}R_1(\psi)}{\mathrm{d}t} = 0 \Rightarrow [A^*] = \frac{k_1^+}{k_1^-} \frac{k_1^+[A][M]}{k_1^-[M] + k_2^+}. \tag{13}$$

Therefore, it is now possible to recover the low and high pressure limits and obtain the following relations similar to Equations (9), (10)

- First order in the PEA high pressure limit

$$k_1^-[M] >> k^+ \Rightarrow \frac{\mathrm{d}[P]}{\mathrm{d}t} = \frac{k_1^+}{k_1^-}k_2^+\frac{k_1^+[A][M]}{k_1^-[M]-k_2^+} = k_2^+\left(\frac{k_1^+}{k_1^-}\right)^2[A]. \tag{14}$$

- The higher orders in the PEA low pressure limit are obtained when complicated dependence of M on, e.g. A, A^* due to liner integrals is taken into account, namely,

$$k_1^-[M] << k^+ \Rightarrow \frac{\mathrm{d}[P]}{\mathrm{d}t} = \frac{k_1^+}{k_1^-}k_2^+\frac{k_1^+[A][M]}{k_1^-[M]+k_2^+} = \frac{\left(k_1^+\right)^2}{k_1^-}[A][M]. \tag{15}$$

Now the question is how all these limits can be treated in such a way that assumptions as well as limits can be rigorously justified, e.g. answer what equations – Equations (9) or (14) and Equations (10) or (15) provide a better approximation of the reduced model?

3.2. *Application of the SPVF*

To answer this question, a particular limit is considered on the same plane taken such that chosen coordinates are not suitable for the SPS consideration. We reformulate the original system by introducing the limit of high pressure above with $\varepsilon := \frac{k_2^+}{k_1^- C_0} << 1$ systems small parameter:

$$\begin{aligned}\frac{\mathrm{d}[A]}{\mathrm{d}t} &= -R_1(\psi) = -k_1^+[A][M] + k_1^-[A^*][M],\\ \frac{\mathrm{d}[A^*]}{\mathrm{d}t} &= R_1(\psi) - R_2(\psi) = k_1^+[A][M] - k_1^-[A^*][M] - \varepsilon k^- C_0[A^*],\end{aligned} \tag{16}$$

The choice of fast and slow sub-fields

$$\Phi(z,\varepsilon) := F(z) + \varepsilon\, G(z) \tag{17}$$

is obvious in this limit by denoting $z = ([A],[A^*])$

$$\begin{aligned}F(z) &:= (-k_1^+[M][A] + k_1^-[M][A^*], k_1^+[M][A] - k_1^-[M][A^*]),\\ G(z) &:= (0, k_1^- C_0[A^*]).\end{aligned} \tag{18}$$

For simplicity and illustration, let us consider $[M] \sim [A]$, which is a good approximation at least at the beginning of the process. By using an additional assumption that the backward and forward reaction constants are equal $k_1^+ = k_1^-$ and considering dimensionless variables as $x = [A]/C_0$ and $y = [A^*]/C_0$ with the fast time scale – $d\sigma = k_1^+ dt$ the original system becomes

$$\begin{aligned}\frac{\mathrm{d}x}{\mathrm{d}\sigma} &= -x(x-y),\\ \frac{\mathrm{d}y}{\mathrm{d}\sigma} &= x(x-y) - \varepsilon y,\end{aligned} \tag{19}$$

with the standard initial condition $x_0 = 1, y_0 = 0$ when no product is present in the initial mixture composition.

It is clear that $F(z) = (-x(x-y), x(x-y))^T$ is a degenerate vector field with the slow manifold defined to the leading order as $\varepsilon \to 0$ by $F(z) = 0$

$$M_{s,0} = \{(x,y) : x - y = 0\}. \tag{20}$$

3.2.1. *Initial data projection in SPVFs with the ILDM*

We will use now the form Equation (19) where both equations are fast in the limit considered. The decomposition of motions exists and is controlled by the system small parameter ε. Suppose we have a scattered initial data and we want to reduce the system. In this case, the initial data must be projected toward the slow curve of the system, given by the zeroth order approximation (Equation 20) (see, e.g. Figure 1). It should be noted that the problem of projection onto slow manifolds is well known and has been treated first mentioned in [25] and referred in the report [26] in chapter 6.5 as 'inclusion of the homogeneous solution'. The original iterative method of the CSP [25] was modified to take into account the fact that during the fast relaxation the system state will evolve along the fast manifolds approximated by the CSP basis of arbitrary order [27, 28] computed at the initial state. By restricting the states on the fast fibers and by using a few Newton iterations, the point on the slow manifold can then be identified. In this way, the so-called radical correction algorithm was established in the CSP method to improve the starting solution of the reduced model and it was implemented, e.g. in [29, 30]. In this respect, the only difference to current study is the observation that the first order of the CSP basis, which corresponds to the ILDM, can be used and computed at the initial data point. This is shown to be sufficient to achieve reliable accuracy for projected state in the considered examples.

The simplest and most straightforward way to implement this is by considering system Jacobi matrix $J_\Phi(z)$, computed at the initial values z_0. Then the fast manifold can be approximated by the eigenspaces of $J_\Phi(z_0)$ [9].

Figure 1 shows typical state plane with its vector field and trajectories starting at different initial conditions, corresponding to varying initial ratios between the main educt and product concentrations that corresponds to changing initial conditions. It is clear that to define an appropriate reduced model as constrained solution onto the slow curve one should project (find relevant) initial data on the slow manifold; one cannot simply keep an initial value to integrate the reduced system. The later might lead to unpredictable results.

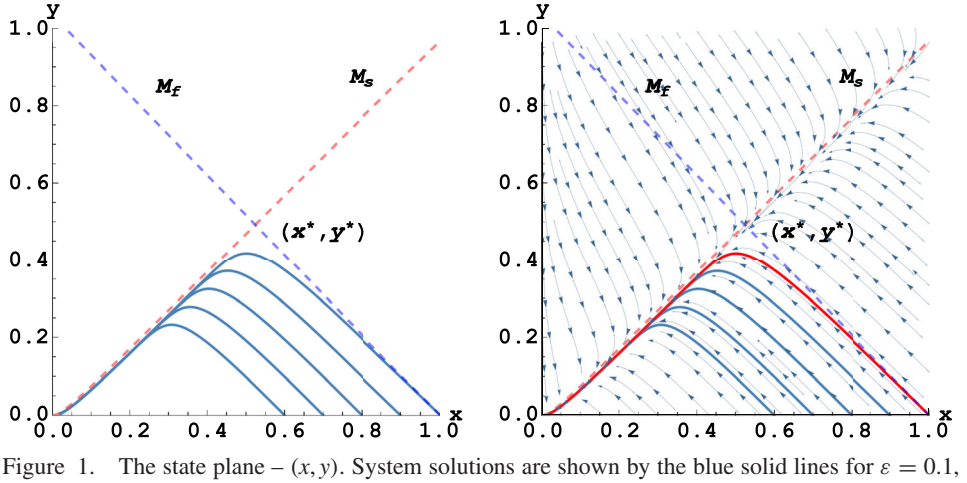

Figure 1. The state plane – (x, y). System solutions are shown by the blue solid lines for $\varepsilon = 0.1$, $x_0 = (0.6, 0.7, 0.8, 0.9, 1.0)$. Streamlines show the system vector field, red dashed line is an approximation for the slow manifold, while blue dashed line is an approximation of the fast manifold based on eigenspaces of the Jacobi matrix at z_0. $(x^*, y^*) = (0.53, 0.48)$ denotes the intersection point of Equation (21) (colour online).

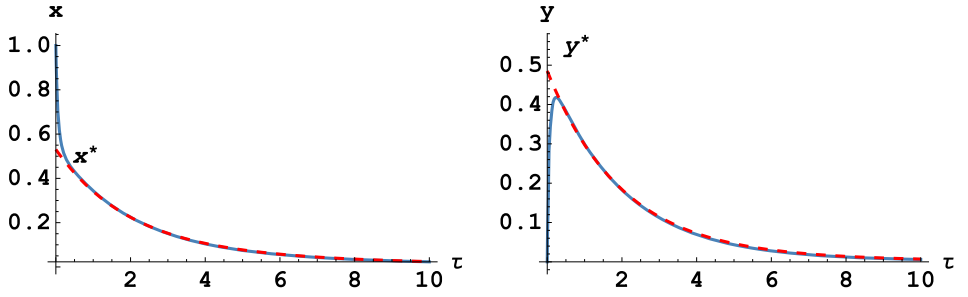

Figure 2. The detailed (solid line) versus reduced (red dashed line) system solutions starting at $z_0 = (1, 0)$ for $\varepsilon = 0.1$. (x^*, y^*) denotes the intersection point of Equation (21) (colour online).

To achieve this, the left eigenvectors of the Jacobi matrix are used to define both an approximation of the fast manifold going through z_0 as well as the slow curve [31, 32] and the intersection $z^* = (x^*, y^*)$ yields the initial data for the system as shown in Figure 2, namely:

$$M_f = \{(x, y) : \tilde{Z}_s(z^* - z_0) = 0\} \cup M_s = \{(x, y) : \tilde{Z}_f \Phi(z^*) = 0\}. \tag{21}$$

In the considered example, time scales are estimated by $J_\Phi(z_0)$ at the initial point $z_0 = (1, 0)$. Eigenvalues are $\lambda_f = -30.3$, $\lambda_s = -0.66$ producing the small parameter estimation at the initial data $\varepsilon_{z_0} = \lambda_s/\lambda_f = 0.021$ with $\tilde{Z}_f = (-0.94, 0.48)$ and $\tilde{Z}_s = (-0.76, -0.73)$ yielding $(x^*, y^*) = (0.53, 0.48)$.

3.2.2. *SPVF and coordinates transformation*

To accomplish the primary goal of the Singular Perturbation Vector Field (SPVF) method, which is to find new coordinates that transforms the original model into a standard Singular Perturbation System (SPS), the explicit fast subfield can be used to redefine the original system. To the leading order the fast subfield in Equation (19) can now be integrated $(dx/dy = -1)$, and the integral curve $u = x + y$ can be used as a slow variable [22] to represent the system in the standard SPS form with, $v := y$ as a fast variable. In the slow time $d\tau = \varepsilon d\sigma$, the standard SPS form yields:

$$\begin{aligned} \frac{\mathrm{d}u}{\mathrm{d}\tau} &= -v, \\ \varepsilon\frac{\mathrm{d}v}{\mathrm{d}\tau} &= (u - v)(u - 2v) - \varepsilon v. \end{aligned} \tag{22}$$

The standard SPS form of the model given by Equation (22) recovers the proper form of Equation (6) when the reactions have different time scales. This form can and can now be used to proceed with model reduction and has no problem with the decomposition. In the leading order, initial data can be projected keeping the slow variable constant $u = u_0 = (x_0 + y_0)$. This, however, will be less accurate since the limit with $\varepsilon = 0.1$ is not asymptotically small and the ILDM will outperform the zeroth order approximation, while the first one will be close to this of the ILDM obtained here [33].

4. Michaelis–Menten model

The second benchmark example, although not directly relevant to the combustion processes, but still represents another benchmark problem for model reduction.

The enzyme kinetics and the model can shed some light on how to treat the system in its dimensional form. An additional motivation to consider this example is to demonstrate and analyse the problem in a dimensional form with strong non-linear behaviour, where the asymptotic limit is not strictly valid. Furthermore, the system is the focus of intensive ongoing investigations in the field of systems biology, both on theoretical and application levels (starting from [18, 28, 30, 34]). Significant efforts have been made to justify the standard asymptotic limits (e.g. Quasi-Steady-State Approximation (QSSA)) in cases where no coordinate fully satisfies the QSSA conditions [30]. We intend to show that SPVF represents the only theoretical basis to treat such systems, which are close to, and even slightly beyond, particular asymptotic limits.

In the case of enzyme kinetics, it was observed that the presence of a small amount of a substance called an enzyme significantly promotes the decomposition of the substrate into the product $S \longrightarrow P$, leading to a non-linear dependence of product formation on substrate concentration [17]. This is exactly the same as the presence of an active radical in a gas mixture enhancing combustion chemistry.

Quite similar to the Lindemann formalism, an extension of the one-step model has been suggested [17]

$$\begin{aligned} S + E &\rightleftharpoons SE \\ SE &\longrightarrow P. \end{aligned} \tag{23}$$

A two-step mechanism in combination with the quasi-steady-state approximation (QSSA) of the complex $C := SE$, helped to explain most of the observations [30]. Moreover, it has become a prevailing tool for modelling the dependence of reaction rate on substrate concentration and for the estimation of reaction rate parameters of the reduced reaction:

$$S \longrightarrow P. \tag{24}$$

The differential equations that are traditionally used to model this situation are

$$\begin{aligned} \frac{\mathrm{d}[E]}{\mathrm{d}t} &= -k_1^+[E][S] + k_1^-[C] + k_2[C], \\ \frac{\mathrm{d}[S]}{\mathrm{d}t} &= k_1^+[E][S] + k_1^-[C] - k_2[C], \\ \frac{\mathrm{d}[C]}{\mathrm{d}t} &= k_1^+[E][S] - k_1^-[C] + k_2[C], \\ \frac{\mathrm{d}[P]}{\mathrm{d}t} &= k_2[C]. \end{aligned} \tag{25}$$

The typical initial conditions are

$$[E] = E_0, \quad [S] = S_0, \quad [C] = 0, \quad [P] = 0.$$

As in the previous model, there are two linear integrals in this system and the system effectively planar, namely,

$$[E](t) + [C](t) = E_0, \quad [S](t) + [C](t) + [P](t) = S_0. \tag{26}$$

Remark These two integrals define a two-dimensional invariant manifold of conserved quantities of the original system. There are at least sixth ways to express the original system on this two-dimensional manifold. All these systems are equivalent, but their representations under different asymptotical limits as degenerate systems can lead to nonequivalent forms and consequently to different conclusions.

In this respect one of the most used and convenient forms to implement the standard QSSA is the following 2D system of the MM model using complex and substrate species

$$\begin{aligned}\frac{\mathrm{d}[S]}{\mathrm{d}t} &= -R_1 = -k_1^+[S]([E]_0 - [C]) + k_1^-[C],\\ \frac{\mathrm{d}[C]}{\mathrm{d}t} &= R_1 - R_2 = k_1^+[S]([E]_0 - [C]) - k_1^-[C] - k_2[C].\end{aligned} \tag{27}$$

4.1. *Standard asymptotic limits of enzyme kinetics*

Following the most complete study of QSSA assumption concerning the system (27), namely, Segel and Slemrod [34] the QSSA for $[C]$ is assumed. The reduced system for substrate concentration and product formation of simplified/reduced model Equation (24) becomes

$$\frac{\mathrm{d}[S]}{\mathrm{d}t} = -R_2 = -k_2\frac{[E]_0[S]}{K_m + [S]}, \tag{28}$$

where the so-called Michaelis–Menten parameter – $K_m = \frac{k_1^- + k_2}{k_1^+}$ appears as a consequence of the QSSA and definition of the slow manifold defined to the leading order by

$$R_1 - R_2 = k_1^+[S]([E]_0 - [C]) - k_1^-[C] - k_2[C] = 0 \iff [C] = \frac{[E]_0[S]}{K_m + [S]}. \tag{29}$$

By using the second linear integral the corresponding equation for the product can be written easily. In the original work of Segal and Stemrod [34] for QSSA was used an additional assumption $E_0 << 1$. The corresponding zero approximation includes $E_0 = 0$, i.e. $\frac{\mathrm{d}[S]}{\mathrm{d}t} = \frac{\mathrm{d}[P]}{\mathrm{d}t} = 0$, see also in Appendix Subsection A.3. It means that QSSA is not directly applicable. The authors used some additional reasoning to avoid this contradiction.

4.2. *Motivation and objective for considering MM*

The question of verification of the QSSA assumption, definition of the system's small parameter and its dependence on the characteristic time scales of different processes involved led to complications that were extensively treated in [34].

In this study, the objective is not to present a reduced model in a certain asymptotic limit, but rather to use asymptotic analysis and the typical orders of the system's parameters to answer how the detailed mechanism (23) can be properly reduced if the original coordinates do not support the standard SPS form. Accordingly, problems of decomposition of motions and fast/slow manifold approximations should become evident.

4.3. *Dimensional approaches, asymptotic limits and conserved subspaces*

To be specific, let us start from the original complete system, where only one linear integral has been used, namely, $[E] + [C] = [E]_0$.

$$\begin{aligned}
\frac{\mathrm{d}[S]}{\mathrm{d}t} &= -R_1 = -k_1^+[S]([E]_0 - [C]) + k_1^-[C], \\
\frac{\mathrm{d}[C]}{\mathrm{d}t} &= R_1 - R_2 = k_1^+[S]([E]_0 - [C]) - k_1^-[C] - k_2[C], \\
\frac{\mathrm{d}[P]}{\mathrm{d}t} &= R_2 = k_2[C].
\end{aligned} \tag{30}$$

The system's second linear integral $[S] + [C] + [P] = [S]_0$ is obvious, but for a while it is kept in the system for the reasons, which should be clarified later.

Following the standard theoretical line, the asymptotic assumption should be implemented for reliable limit to be considered and, hence, dimensionless form can be developed to reduce the number of system parameters and variables. This way real system dimension in parameters and variables space can be identified and used for further investigations and understanding the considered process and delineating the typical system dynamics and variety of different regimes.

So far, in the original detailed model, we have five physical parameters – $[S]_0, [E]_0, k_1^+, k_1^-, k_2$ and three variables $[S], [C], [P]$. The typical asymptotic limit of the system considered here arises from differences in enzyme and substrate concentrations $[S]_0 >> [E]_0$ and reaction rates $k_1^+[E]_0 \sim k_1^- >> k_2$. This leads to a natural inherent hierarchy within the system. The dimensionless form can be constructed using natural scaling for variables

$$(s, c, p) = ([S]/[S]_0, [C]/[E]_0, [P]/[S]_0)$$

and rates. Using the limiting reaction rate for the time – $d\tau = k_2 dt$, we obtain the dimensionless form of the system (30) as

$$\begin{aligned}
\frac{\mathrm{d}s}{\mathrm{d}\tau} &= -1/\delta((1-c)s - \eta c), \\
\epsilon\frac{\mathrm{d}c}{\mathrm{d}\tau} &= 1/\delta((1-c)s - \eta c) - \epsilon c, \\
\frac{\mathrm{d}p}{\mathrm{d}\tau} &= \epsilon c,
\end{aligned} \tag{31}$$

which should be considered with the standard initial conditions

$$(s, c, p) = (1, 0, 0).$$

The choice of scaling is natural simply because of the linear integrals provide estimates $max[C] < [E]_0$ and $max[P] < [S]_0$.

One obvious small parameter emerges

$$\epsilon = [E]_0/[S]_0 << 1.$$

In this case, the linear integral is represented in the form

$$s + \epsilon c + p = 1. \tag{32}$$

Additionally two more dimensionless parameters need to be specified:

$$\delta = k_2/(k_1^+[E]_0) << 1,$$

which is the ratio of the second and first-forward reaction rates and

$$\eta = k_1^-/(k_1^+[S]_0) \sim O(1),$$

relevant to the first backward and forward reaction rates.

Note that the linear integral now Equation (32) is senseless for the zero approximation of the invariant manifold $\epsilon \to 0$. It means the linear integral degenerates in this asymptotic limit. It can be corrected by three ways: using the first approximation; formally distinguish singular and regular perturbation, using an another representation of the original model on the manifold, for example, by using species $(s,\ p)$. Of course all representations are equivalent but its asymptotic analysis can lead to different conclusions. We will discuss in details all these three ways.

Note that the second parameter can also be large or small, depending on the internal hierarchy in the first reaction. For now, we will consider it to be of order one. However it is ease to see that it might also be small enough, i.e.

$$\eta = k_1^-/(k_1^+[E]_0)[E]_0/[S]_0 = k_1^-/(k_1^+[E]_0)\epsilon.$$

This is especially true if we keep in mind the basic assumption – $k_1^- \sim k_1^+[E]_0$. Three parameters describe

- ϵ – difference in concentrations;
- δ – ratio of the rate of the first forward reaction to the rate of the second limiting one;
- η – weighted ratio of the rates of the first forward and backward reactions.

The form of the system (31), (33) can now be used to explain observations made where the standard limit is valid. In this case, there is a bi-hierarchy resulting in product formation that is several orders of magnitude slower than the balance between substrate and complex. Furthermore, the rate of change of the substrate can be neglected at the leading order once the balance between the first backward and forward reactions is established. Such that even if δ is considered as an additional singular perturbation parameter, the situation may become more acute, but it does not significantly change the outcome of the analysis. Therefore, δ might be kept at an order of unity compared to the differences in the concentrations, which defines the system small parameter to the leading order.

The last system has two perturbations with the same parameter ϵ singular and regular. The singular perturbation is responsible for fast reaction in the initial period (fast motion) and the regular perturbation is responsible for the product formation. Formally, it will

be more reasonable to use different notations for both perturbations: ϵ for the singular perturbation and ϵ_1 for the regular one.

$$\begin{aligned}\frac{\mathrm{d}s}{\mathrm{d}\tau} &= -1/\delta((1-c)s-\eta c),\\ \epsilon\frac{\mathrm{d}c}{\mathrm{d}\tau} &= 1/\delta((1-c)s-\eta c)-\epsilon_1 c,\\ \frac{\mathrm{d}p}{\mathrm{d}\tau} &= \epsilon_1 c,\end{aligned} \tag{33}$$

Therefore instead of usual scale of approximations of the slow manifold (curve), we have more flexible row of approximations for the (ϵ, ϵ_1) pair, i.e. (0,0)-approximation, (0,1)-approximation, (1,1)-approximation. It seems that (0,1)-approximation is reasonable for QSSA analysis, see also Subsection A.2 in Appendix, where further analytical estimate for the first-order approximation of the slow curve is given. For example, the (0,1)-slow curve is the following:

$$1/\delta((1-c)s-\eta c)-\epsilon_1 c = 0.$$

Additionally, the third equation of the system (Equation 33) decouples from two other equations. Hence, the slow invariant curve can be obtained by the standard SPS technique leading to the slow manifold equation to the first order given by

$$c(s) = \frac{s}{s+\eta}\left(1-\epsilon\frac{\delta}{s+\eta}\right). \tag{34}$$

The latter confirms the leading order of the standard QSSA-based reduced model (Equation 27). When product, e.g. substrate, is only measured in experiments, no additional information can be obtained about the rates and all three parameters needed to be specified for developing the detailed model. In this case, there are only two becomes available, namely, the ratio of the rates of the first forward and backward reactions due to η and second reaction rate constant due to characteristic time scales. In order to be able to estimate the rate of first reaction δ is needed. For this the detailed information on the fast transient in terms of the complex behaviour should be provided since the substrate is also a slow variable with respect to the complex in the considered limit. Alternatively, if one has a situation when the first order in Equation (34) is significant, then the correction to the slow curve becomes important and the estimate for δ has to be provided as well. This, however, is not feasible in the considered limit. In this case

$$\epsilon\delta = [E]_0/[S]_0\ k_2/(k_1^+[E]_0) = k_2/(k_1^+[S]_0) << 1.$$

The case of non-linear transformation in frequently considered limit is shortly outlined in Appendix Subsection A.3. In the following, however, linearly decomposed vector field is considered in for this benchmark in the dimensional form under consideration of a weak asymptotic limit discussed above.

4.4. *Benchmark example of the weak asymptotic limit*

In their seminal 2001 paper, Roussel and Fraser [18] used a different set of coordinates, namely (s,p), to represent the planar system after a detailed analysis of the previous QSSA

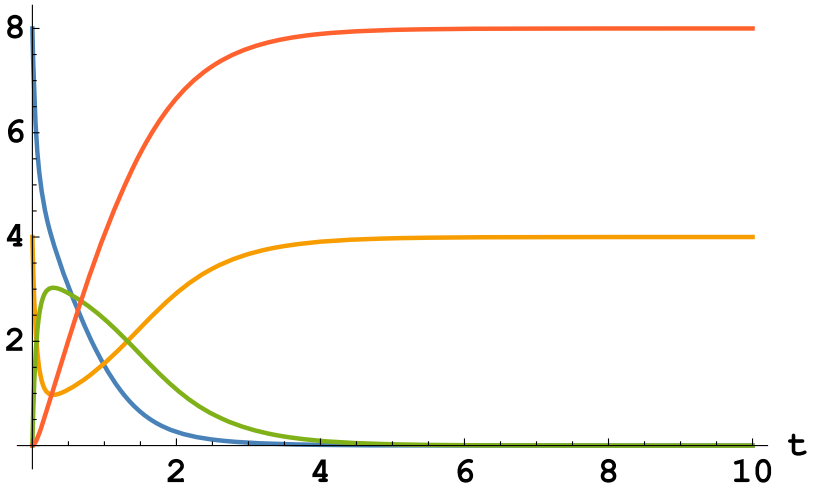

Figure 3. System solution of Equation (25) for the initial point $(S_0, p_0, E_0, c_0) = (8, 0, 4, 0)$ (colour online).

approximation. In their model, both equations shared the same time scales. The SPVF analysis performed below avoids these technical difficulties through a corresponding transformation of coordinates using the ILDM approach similar to the previous section. Note that the appendix constructs a nonlinear fiber bundle, which can be used in distinguished asymptotic limit to improve accuracy to the first-order approximation provided by the ILDM [33].

Additionally, the system is considered in the dimensional form showing the scaling invariance of the ILDM with respect to estimation of the decomposition present in the system. Accordingly, the original system (Equation 25) is considered here with commonly used illustrative parameter set – $\{k_1^+ = 2,\ k_1^- = 1,\ k_2 = 1.5,\ [E]_0 = 4,\ [S]_0 = 8\}$. For considered set of physical parameters, the dimensionless parameters become $\varepsilon = 0.5,\ \delta = 0.18,\ \eta = 0.06$.

The detailed solution profiles are shown in Figure 3. Although there is no evident scaling differences in the parameter set used, one sees two stage behaviour of the system solution variables, after about $t = 0.25\ s$ the relatively fast motion is over and relatively slow dynamics in terms of variables changes is observed.

Figure 4 shows the state plane in the (s, p) projection with a number of system solution trajectories having different initial points, but yielding same conserved quantity - $s_0^* + p_0^* = s_0$. These are taken to yield the same equilibrium and to show how relatively fast part of the system solution trajectory looks like. After the transient stage all solution trajectories are merging signifying the slow manifold existence.

4.5. *Initial data projection with the ILDM*

Now, the ILDM is applied once again at the initial point similar to the Lindemann case (Equation 21) yielding approximations for both slow and fast manifolds in the considered $z = (s, p)$ plane. In this example, time scales are estimated by $J_\Phi(z_0)$ at the initial point $z_0 = (s_0, 0)$. Eigenvalues are $\lambda_f = -26.03,\ \lambda_s = -0.46$ producing the small

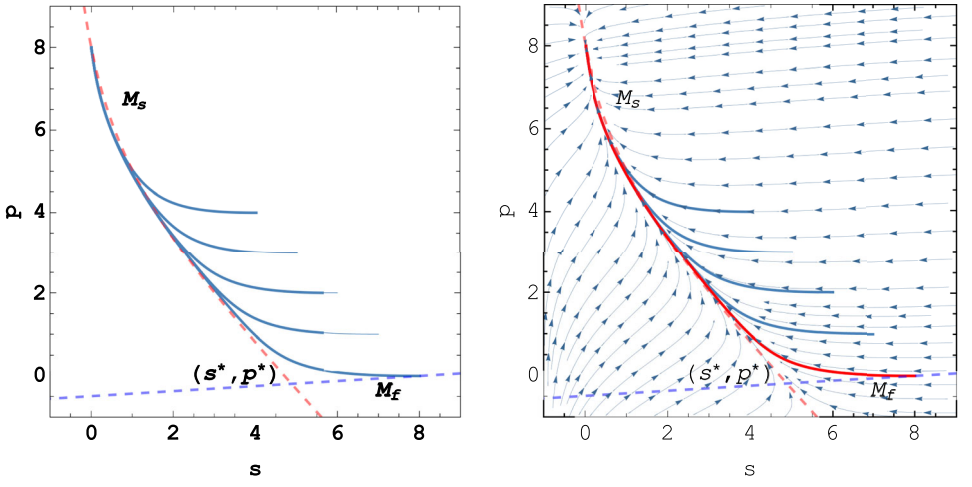

Figure 4. The state plane – (s,p). System solutions are shown by the blue solid lines for $s_0^* + p_0^* = s_0$, $s_0^* = (8,7,6,5,4)$. Streamlines show the system vector field, red dashed line is an approximation for the slow manifold, while blue dashed line is an approximation of the fast manifold based on eigenspaces of the Jacobi matrix at z_0. (s^*, p^*) denotes the intersection point of Equation (21) for the initial point $(s_0, p_0) = (8,0)$ (colour online).

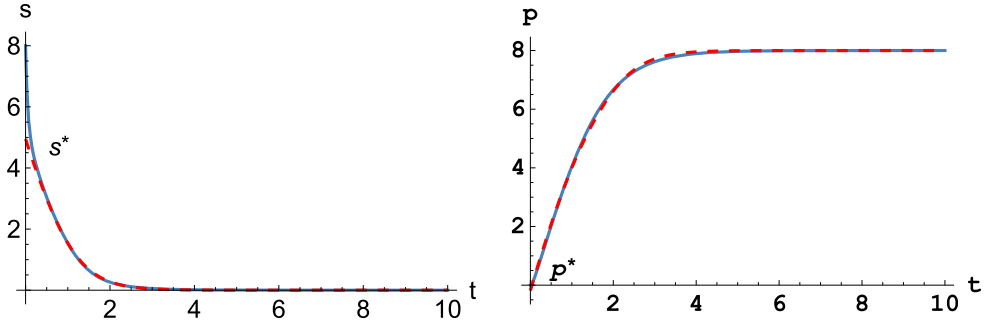

Figure 5. The detailed (solid line) versus reduced (red dashed line) system solutions starting at $z_0 = (8,0)$ and (s^*, p^*) denotes the intersection point of Equation (21) (colour online).

parameter estimation at the initial data $\varepsilon_{z_0} = \lambda_s/\lambda_f = 0.018$ with $\tilde{Z}_f = (-0.96, -0.66)$ and $\tilde{Z}_s = (-0.07, -1.16)$ yielding $(s^*, p^*) = (4.95, -0.19)$.

This is illustrated also in Figure 4, where by intersection of the slow and fast manifolds an initial state for reduced model is defined. Although the asymptotic limit is not well justified still due to non-linearity of the vector field, the decomposition exists and, moreover, it is captured successfully by the modified ILDM, $\varepsilon_{z_0} = 0.018$. This represents a very important observation and confirm the robustness of the suggest approach showing proper asymptotic can be valid slightly beyond assumed limits. Figure 5 shows the performance of the reduced versus detailed system solutions once the initial point is found and the ILDM approximation for the slow invariant manifold is considered. In this comparison, the accuracy remains quite high in spite the fact the asymptotic limit exists but cannot be accessed by studying physical system parameters and initial conditions only.

5. Conclusion

In this paper, the questions of automatic detection of appropriate asymptotic limits, choice of system representation for model reduction are revisited in a very simple but meaningful and important benchmark models. These are typically used to illustrate and to describe multiple-scale behaviour of chemically reacting systems. Moreover, these represent basic and fundamental building blocks to construct complicated networks/models of chemical kinetics in various fields of chemical reaction engineering.

It is demonstrated how the framework of SPVFs can redefine the decomposition and subsequently the reduced model. The key element in the theory and in applications is the family of fast manifolds, which can reconcile the decomposition problem. The modified ILDM computed on the initial data is also shown to help in the estimation and approximation of these fast manifolds. Thus it becomes extremely useful for both manifold definition and initial data projection.

The Lindemann model was used to illustrate how the theory can be implemented if no appropriate representation is available, i.e. both variables are fast. While the Michaelis–Menten model was used to demonstrate a weak asymptotic limit and show how the suggested combination (SPVFs and ILDMs) is implemented and performs being applied to the system in the dimensional form. In both cases, the suggested combination overcomes both theoretical and technical difficulties in these important benchmark models.

Author contributions

CRediT: **Viatcheslav Bykov:** Conceptualization, Data curation, Formal analysis, Investigation, Methodology; **Vladimir Goldshtein:** Conceptualization, Formal analysis, Supervision

Disclosure statement

No potential conflict of interest was reported by the author(s).

Funding

The authors acknowledge the financial support provided by the Deutsche Forschungsgemeinschaft (DFG), within SFB TRR 150, TP B07 – Project number 237267381.

ORCID

Viatcheslav Bykov http://orcid.org/0000-0002-2274-8410

References

[1] T. Poinsot, S. Candel, and A. Trouvé, *Applications of direct numerical simulation to premixed turbulent combustion*, Prog. Energy Combust. Sci. 21(6) (1995), pp. 531–576. https://doi.org/10.1016/0360-1285(95)00011-9.

[2] S. Posch, C. Gößnitzer, M. Lang, R. Novella, H. Steiner, and A. Wimmer, *Turbulent combustion modeling for internal combustion engine cfd: A review*, Prog. Energy Combust. Sci. 106 (2025), pp. 101200. https://doi.org/10.1016/j.pecs.2024.101200.

[3] S.A. Hosseini, P. Boivin, D. Thévenin, and I. Karlin, *Lattice Boltzmann methods for combustion applications*, Prog. Energy Combust. Sci. 102 (2024), pp.101140. https://doi.org/10.1016/j.pecs.2023.101140.

[4] F. Egolfopoulos, N. Hansen, Y. Ju, K. Kohse-Höinghaus, C. Law, and F. Qi, *Advances and challenges in laminar flame experiments and implications for combustion chemistry*, Prog. Energy Combust. Sci. 43 (2014), pp. 36–67. https://doi.org/10.1016/j.pecs.2014.04.004.
[5] J. Warnatz, U. Maas, and R. Dibble, *Combustion: Physical and Chemical Fundamentals, Modeling and Simulation, Experiments, Pollutant Formation*, 4th ed., Springer, Berlin, Heidelberg, 2006.
[6] D.A. Goussis and U. Maas, *Model reduction for combustion chemistry*, in *Turbulent Combustion Modeling*, 2011, pp. 193–220.
[7] T. Turányi and A.S. Tomlin, *Analysis of Kinetic Reaction Mechanisms*, Vol. 20, Springer, 2014.
[8] N. Peters, *Laminar diffusion flamelet models in non-premixed turbulent combustion*, Prog. Energy Combust. Sci. 10(3) (1984), pp. 319–339.
[9] U. Maas and S.B. Pope, *Simplifying chemical kinetics: Intrinsic low-dimensional manifolds in composition space*, Combust. Flame 88(3-4) (1992), pp. 239–264.
[10] S. Lam and D. Goussis, *Understanding complex chemical kinetics with computational singular perturbation*, Symp. Combust. 22(1) (1989), pp. 931–941. https://doi.org/10.1016/S0082-0784(89)80102-X.
[11] V. Bykov and U. Maas, *The extension of the ildm concept to reaction–diffusion manifolds*, Combust. Theor. Model. 11(6) (2007), pp. 839–862. https://doi.org/10.1080/13647830701242531.
[12] S. Borok, I. Goldfarb, and V. Gol'dshtein, *Causes for 'ghost' manifolds*, Commun. Nonlinear Sci. Numer. Simul. 14(5) (2009), pp. 1791–1795. https://doi.org/10.1016/j.cnsns.2008.06.010.
[13] N. Fenichel, *Geometric singular perturbation theory for ordinary differential equations*, J. Differ. Equ. 31(1) (1979), pp. 53–98. https://doi.org/10.1016/0022-0396(79)90152-9.
[14] V. Bykov, V. Gol'dshtein, and U. Maas, *Simple global reduction technique based on decomposition approach*, Combust. Theory Model. 12(2) (2008), pp. 389–405.
[15] V. Bykov, I. Goldfarb, and V. Gol'dshtein, *Singularly perturbed vector fields*, J. Phys. Conf. Ser. 55(1) (2006), pp. 28. https://doi.org/10.1088/1742-6596/55/1/003.
[16] F.A. Lindemann, S. Arrhenius, I. Langmuir, N.R. Dhar, J. Perrin, and W.C. McC. Lewis, *Discussion on 'the radiation theory of chemical action'*, Trans. Faraday Soc. 17 (1922), pp. 598–606. https://doi.org/10.1039/TF9221700598.
[17] L. Michaelis and M.L. Menten, *The kinetics of the inversion effect*, Biochem. Z 49 (1913), pp. 333–369.
[18] M.R. Roussel and S.J. Fraser, *Invariant manifold methods for metabolic model reduction*, Chaos: Interdisciplinary J. Nonlinear Sci. 11(1) (2001), pp. 196–206. https://doi.org/10.1063/1.1349891.
[19] M. Bodenstein, *Eine theorie der photochemischen reaktionsgeschwindigkeiten*, Z. Phys. Chem. 85(1) (1913), pp. 329–397.
[20] J. Bowen, A. Acrivos, and A. Oppenheim, *Singular perturbation refinement to quasi-steady state approximation in chemical kinetics*, Chem. Eng. Sci. 18(3) (1963), pp. 177–188. https://doi.org/10.1016/0009-2509(63)85003-4.
[21] A. Tikhonov, *Sistemy differentsial'nykh uravneniy soderzhashchikh malyye parametry pri proizvodnykh [systems of differential equations containing small parameters at the derivatives]*, Mat. Sb. (NS) 31(73) (1952), pp. 575–586.
[22] V. Bykov and V. Gol'dshtein, *Fast and slow invariant manifolds in chemical kinetics*, Comput. Math. Appl. 65(10) (2013), pp. 1502–1515. grasping Complexity. https://doi.org/10.1016/j.camwa.2013.01.040.
[23] Y. Cherkinsky, *Singularly perturbed vector fields*, PhD thesis, Ben-Gurion University of the Negev, Beer-Sheva, Israel, 2022. Available at https://cris.bgu.ac.il/en/studentTheses/singularly-perturbed-vector-fields-2.
[24] Y. Zeldovich and G. Barenblatt, *Theorv of flame propagation*, Combust. Flame 3 (1959), pp. 61–74. https://doi.org/10.1016/0010-2180(59)90007-0.
[25] S.H. Lam and D.A. Coussis, *Conventional Asymptotics and Computational Singular Perturbation for Simplified Kinetics Modelling*, Springer, Berlin, Heidelberg, 1991. pp. 227–242. https://doi.org/10.1007/BFb0035372.
[26] S.H. Lam, *Computational reacting gas dynamics*, NASA Contractor Report NASA-CR-193073, NASA Center for Aerospace Information (CASI), United States, report No. 19930010670, Accession No. 93N19859, 1993. Available at https://ntrs.nasa.gov/citations/19930010670.

[27] M. Valorani, D.A. Goussis, F. Creta, and H.N. Najm, *Higher order corrections in the approximation of low-dimensional manifolds and the construction of simplified problems with the csp method*, J. Comput. Phys. 209(2) (2005), pp. 754–786. https://doi.org/10.1016/j.jcp.2005.03.033.
[28] D.A. Goussis, *Quasi steady state and partial equilibrium approximations: Their relation and their validity*, Combust. Theory Model. 16(5) (2012), pp. 869–926. https://doi.org/10.1080/13647830.2012.680502.
[29] J.M. Ortega, H.N. Najm, J. Ray, M. Valorani, D.A. Goussis, and M. Frenklach, *Adaptive chemistry computations of reacting flow*, J. Phys. Conf. Ser. 78(1) (2007), pp. 012054. https://doi.org/10.1088/1742-6596/78/1/012054.
[30] D.G. Patsatzis and D.A. Goussis, *A new michaelis-menten equation valid everywhere multiscale dynamics prevails*, Math. Biosci. 315 (2019), pp. 108220. https://doi.org/10.1016/j.mbs.2019.108220.
[31] V. Bykov, C. Yu, V. Gol'dshtein, and U. Maas, *Model reduction and mechanism comparison of hydrogen/oxygen auto-ignition*, Proc. Combust. Inst. 37(1) (2019), pp. 781–787. https://doi.org/10.1016/j.proci.2018.06.189.
[32] C. Yu, V. Bykov, and U. Maas, *Coupling of simplified chemistry with mixing processes in pdf simulations of turbulent flames*, Proc. Combust. Inst. 37(2) (2019), pp. 2183–2190. https://doi.org/10.1016/j.proci.2018.05.126.
[33] H.G. Kaper and T.J. Kaper, *Asymptotic analysis of two reduction methods for systems of chemical reactions*, Phys. D: Nonlinear Phenom. 165(1) (2002), pp. 66–93. https://doi.org/10.1016/S0167-2789(02)00386-X.
[34] L.A. Segel and M. Slemrod, *The quasi-steady-state assumption: A case study in perturbation*, SIAM Rev. 31(3) (1989), pp. 446–477. https://doi.org/10.1137/1031091.

Appendix. Non-linear SPVF analysis and first-order approximation

A.1. *Lindemann model, linear integrals*

The reaction mechanism characteristic constants are

$$n_r = 2, \quad n_s = 4, \quad k_2^- = 0,$$

with a simple stoichiometric matrix

$$\mathbf{S} = \begin{pmatrix} -1 & 0 \\ 0 & 0 \\ 1 & -1 \\ 0 & 1 \end{pmatrix}. \tag{A1}$$

The following mathematical model, which is established and detailed elsewhere [16] is reproduced here for completeness and educational purposes. This aims to help readers to grasp the essence of the idea and concept suggested, namely:

$$\frac{\mathrm{d}\psi}{\mathrm{d}t} = \begin{pmatrix} -1 & 0 \\ 0 & 0 \\ 1 & -1 \\ 0 & 1 \end{pmatrix} \begin{pmatrix} R_1(\psi) \\ R_2(\psi) \end{pmatrix} = \begin{pmatrix} -k_1^+[A][M] + k_1^-[A^*][M] \\ 0 \\ k_1^+[A][M] - k_1^-[A^*][M] - k_2^+[A^*] \\ k_2^+[A^*] \end{pmatrix}. \tag{A2}$$

The two trivial linear integrals of the system (Equation A2) are determined by the rank of the matrix **S**. These linear integrals are important for the reduction of dimension of the model system. It can be seen that, by construction, the first trivial integral is given by the expression

$$\frac{\mathrm{d}[M]}{\mathrm{d}t} = 0, \quad [M] = const. \tag{A3}$$

This means that the third-body concentration does not change during these elementary reactions. The second linear integral must exist, since the rank of the stoichiometric matrix **S** is 2. Indeed, by summation all equations up, one obtains

$$\frac{\mathrm{d}[A]}{\mathrm{d}t} + \frac{\mathrm{d}[A^*]}{\mathrm{d}t} + \frac{\mathrm{d}[P]}{\mathrm{d}t} = 0, \; [A] + [A^*] + [P] = [A]_0 + [A^*]_0 + [P]_0 := C_0. \tag{A4}$$

Here, quantities $[A]_0, [A^*]_0, [P]_0$ are initial data.

A.2. *First-order approximation – Michaelis–Menten*

We start with the system presentation by Equation (27). The very same result can be obtained when $([P], [S])$ are used instead similar as, e.g. in Lindemann model. The key is assumption about rate of processes involved, namely, one can assume the first reaction is a fast one, while the second defines a rate limiting reaction – $R_1 \gg R_2$ or vice versa. In the first most common case, both equations represent the fast motion and are singularly perturbed. Then according to the SPVF theory, one can define suitable coordinates to decompose the vector field – $F = F_f + F_s$, with $F_f = (-R_1, R_1)$; $F_s = (0, R_2)$ and obtain $[C]$ for fast and $[C] + [S]$ for slow one. At this stage, one can employ the QSSA and recover (28) with slow manifold (29). But let us follow strictly the theory which says in zero order approximation the slow manifold is defined by F_f

$$R_1 = k_1^+[S]([E]_0 - [C]) - k_1^-[C] = 0 \iff [C] = \frac{[E]_0[S]}{\frac{k_1^-}{k_1^+} + [S]}, \tag{A5}$$

and then in the zero-order approximation the system (28) holds, but with $K_m = \frac{k_1^-}{k_1^+}$. While the first-order correction, which can be obtained to the leading order by invariance condition, namely, via standard differentiation of the zero order approximation along the vector field

$$\frac{\mathrm{d}R_1}{\mathrm{d}t} = 0 \iff \frac{\partial R_1}{\partial [S]}\frac{\mathrm{d}[S]}{\mathrm{d}t} + \frac{\partial R_1}{\partial [C]}\frac{\mathrm{d}[C]}{\mathrm{d}t} = 0, \tag{A6}$$

$$\left(1 + \frac{k_1^+([E]_0 - [C])}{k_1^+[S] + k_1^-}\right)(k_1^+[S]([E]_0 - [C]) - k_1^-[C]) - k_2[C] = 0. \tag{A7}$$

In this correction, one can see that the original idea of QSSA approximates the first-order correction of the manifold when $\frac{([E]_0 - [C])}{[S] + K_m} \ll 1$, which is actually similar to Equation (81) from [34]. An estimation for $\delta_S = \frac{[E]_0}{[S]_0 + K_m} \ll 1$ in [34] is given with estimation by initial values, namely, $[C] \to 0$, $[S] \to [S]_0$ and standard definition can now be recovered – K_m.

The correction term found in (A6) can be used to support the standard QSSA assumption. It can be taken into account when reaction rate parameters are estimated and the model is fitted to the experimental data. This might be extremely useful in situations when the asymptotic limit is not strictly attained. This poses an interesting question to the follow-up studies on modelling experimental transient or steady data.

An additional remark concerns the other asymptotic limit of $R_2 \gg R_1$ a very similar approach can be used to single out the leading order and more important first-order correction to the slow invariant manifold. Though in this case, the second reaction has to be considered as an elementary reaction.

A.3. *Non-linear SPVFs – Michaelis–Menten*

Consider the Michaelis–Menten model using observable variables substrate s and product p to represent the system. The corresponding model is as follows:

$$\begin{aligned} \frac{\mathrm{d}s}{\mathrm{d}t} &= -k_1^+ e_0 s + (k_1^+ s + k_1^-)(s_0 - (s + p)) \\ \frac{\mathrm{d}p}{\mathrm{d}t} &= k_2(s_0 - (s + p)) \end{aligned} \tag{A8}$$

The initial data are $s(0) = s_0, p(0) = 0$. Under normal circumstances $e_0 << 1$.

The system has the unique stationary point $s = 0, p = s_0$.

The system trajectories are solutions of the ordinary differential equation

$$\frac{\mathrm{d}p}{\mathrm{d}s} = \frac{k_2(s_0 - (s + p))}{-k_1^+ e_0 s + (k_1^+ s + k_1^-)(s_0 - (s + p))}. \tag{A9}$$

The non-linear version of the SPVF algorithm is relevant here. This means that we are looking for a non-linear change of coordinates that transforms the original system to a singularly perturbed one.

Slow nonlinear part of the original vector field is as follows:

$$\frac{\mathrm{d}u}{\mathrm{d}t} := \frac{1}{k_1^+}\left[\frac{k_2}{k_1^+ s + k_1^-}\frac{\mathrm{d}s}{\mathrm{d}t} - \frac{\mathrm{d}p}{\mathrm{d}t}\right].$$

The new slow variable u can be easily calculated as

$$u(s,p) = \frac{k_2}{(k_1^+)^2} ln(k_1^+ s + k_1^-) - \frac{p}{k_1^+}.$$

The new fast variable v is orthogonal to the new slow variable u. Here is a relevant representation:

$$\frac{\mathrm{d}v}{\mathrm{d}t} = \frac{1}{k_1^+}\left[\frac{k_1^+ s + k_1^-}{k_2}\frac{\mathrm{d}s}{\mathrm{d}t} + \frac{\mathrm{d}p}{\mathrm{d}t}\right].$$

The new fast variable v can be easily calculated as

$$v(s,p) = \frac{k_1^+ s^2 + k_1^- s}{k_1^+ k_2} - p.$$

Let us detail the justification for the division of new variables into slow and fast. Let's begin by considering the slow variable u as it's defined in the original variables:

$$\frac{\mathrm{d}u}{\mathrm{d}t} = -\frac{k_2}{k_1^+ s + k_1^-} e_0 s.$$

The function $\frac{k_2}{k_1^+ s + k_1^-}$ is a monotone growing one. Its maximal value is $\frac{k_2}{k_1^+ s_0 + k_1^-}$. Because $e_0 << 1$ the new variable u is a slow variable.

By similar simple calculations for v, we obtain

$$\frac{\mathrm{d}v}{\mathrm{d}t} = -e_0 s + \left[\frac{k_1^+ s + k_1^-}{k_1^+} + \frac{k_2^2}{(k_1^+)^2 s + k_1^+ k_1^-}\right](s_0 - (s+p)).$$

Therefore the new variable v is a fast variable.

The slow curve $\frac{\mathrm{d}v}{\mathrm{d}t} = 0$ takes the form $s + p = s_0$ in the zero approximation. The (0,1)-approximation is as follows:

$$0 = -e_0 s + \left[\frac{k_1^+ s + k_1^-}{k_1^+} + \frac{k_2^2}{(k_1^+)^2 s + k_1^+ k_1^-}\right](s_0 - (s+p)). \tag{A10}$$

It's more informative, just like the previous model was.

We note that Segal and Slemrod [34] have used an additional assumption for their QSSA approximation $s_0 - (s+p) \approx 0$. It is the null-cline for $\frac{\mathrm{d}p}{\mathrm{d}t}$, and naturally leads to the conclusion that $\frac{\mathrm{d}p}{\mathrm{d}t} = 0$.

The (0,1)-approximation of the slow motion along the slow curve is

$$\frac{\mathrm{d}u}{\mathrm{d}t} := -\frac{k_2}{k_1^+ s + k_1^-}\epsilon s.$$

Let us remark that the equation for trajectories is the following:

$$p(s) = \frac{k_2}{k_1^+} ln(k_1^+ s + k_1^-) + k_2^2 \epsilon_0 \int_0^s \frac{s}{k_1^+ s(s_0 - (s+p)(k_1^+ s(k_1^-)^2 - k_1^+ s\epsilon_0))} + const.$$